SOURCE
DATA

TRANSPARENT
PROCESS

EMBO *reports*

Mouse endothelial OTUD1 promotes angiotensin II-induced vascular remodeling by deubiquitinating SMAD3

Zhuqi Huang[1,2], Sirui Shen[1,2], Mengyang Wang[1], Weixin Li[1], Gaojun Wu[2], Weijian Huang[2], Wu Luo[1] & Guang Liang[1,2,3,*] (iD)

Abstract

Understanding the molecular mechanisms of pathological vascular remodeling is important for treating cardiovascular diseases and complications. Recent studies have highlighted a role of deubiquitinases in vascular pathophysiology. Here, we investigate the role of a deubiquitinase, OTUD1, in angiotensin II (Ang II)-induced vascular remodeling. We detect upregulated OTUD1 in the vascular endothelium of Ang II-challenged mice and show that OTUD1 deletion attenuates vascular remodeling, collagen deposition, and EndMT. Conversely, OTUD1 overexpression aggravates these pathological changes both *in vivo* and *in vitro*. Mechanistically, SMAD3 is identified as a substrate of OTUD1 using co-immunoprecipitation followed by LC–MS/MS. We find that OTUD1 stabilizes SMAD3 and facilitates SMAD3/SMAD4 complex formation and subsequent nuclear translocation through both K48- and K63-linked deubiquitination. OTUD1-mediated SMAD3 activation regulates transcription of genes involved in vascular EndMT and remodeling in HUVECs. Finally, SMAD3 inhibition reverses OTUD1-promoted vascular remodeling. Our findings demonstrate that endothelial OTUD1 promotes Ang II-induced vascular remodeling by deubiquitinating SMAD3. We identify SMAD3 as a target of OTUD1 and propose OTUD1 as a potential therapeutic target for diseases related to vascular remodeling.

Introduction

Vascular remodeling is a major problem associated with hypertension and is considered as a precursor to the development of microvascular and macrovascular complications, such as cardiovascular and renal complications (Laurent & Boutouyrie, 2015). Hypertensive vascular remodeling that occurs in response to persistently elevated blood pressure is characterized by vascular fibrosis, extracellular matrix deposition and dysfunction of smooth muscle and endothelium, resulting in altered vascular resistance that affects both local and systemic hemodynamics (Schiffrin & Touyz, 2004). Thus, pathological vascular remodeling is an imperative target for cardiovascular therapy. Recent studies have shown that increased level of angiotensin II (Ang II), the major effector in the renin–angiotensin system, is capable of mediating hypertensive vascular remodeling (Forrester *et al*, 2018). Ang II plays a central role in the development of hypertension and hypertensive vascular remodeling. These activities have been reported to involve the induction of endothelial-to-mesenchymal transition (EndMT; Zeisberg *et al*, 2007). However, up till now the molecular mechanisms and clinical treatment of hypertensive vascular EndMT are poorly known. Therefore, identifying innovative regulatory molecules of Ang II-induced pathological vascular remodeling and elucidating their mechanisms of action have great scientific implications and clinical value and may provide potential targets for treating vascular remodeling-related diseases.

Ubiquitination is a common and reversible post-transcriptional modification that regulates numerous cellular actions, including cell signal transduction and fate determination (Popovic *et al*, 2014). Protein ubiquitination is a three-step enzymatic catalysis process involving ubiquitin-activating enzymes (E1), ubiquitin-conjugating enzymes (E2) and ubiquitin ligases (E3). E3 regulate the specificity of this reaction and the types of ubiquitin linkages on substrates through the amino acid residues M1, K6, K11, K27, K29, K33, K48, and K63, thus determining the fate of the substrates (Komander & Rape, 2012). In contrast, deubiquitinases (DUBs) catalyze the removal of ubiquitin from proteins. DUBs also perform multiple biological functions by modulating different substrates to precisely

1   Chemical Biology Research Center, School of Pharmaceutical Sciences, Wenzhou Medical University, Wenzhou, China
2   Department of Cardiology, The First Affiliated Hospital of Wenzhou Medical University, Wenzhou, China
3   School of Pharmaceutical Sciences, Hangzhou Medical College, Hangzhou, China
    *Corresponding author. Tel/Fax: +86 577 86699396; E-mail: wzmcliangguang@163.com

regulate protein function, localization, and degradation (Senft *et al*, 2018). To date, approximately 100 DUBs have been discovered in human and they regulate intracellular signal transduction and the pathogenesis and development of various diseases, such as cancer, infectious diseases, and cardiovascular diseases (Harrigan *et al*, 2018).

Ovarian tumor deubiquitinase 1 (OTUD1), which belongs to the OTU protein family, is a DUB that has been reported to participate in the progression of some diseases. Previous studies have reported that OTUD1 regulates innate immune response (Lu *et al*, 2018; Zhang *et al*, 2018). Daisuke *et al* found that OTUD1 regulates NF-κB and KEAP1-mediated inflammation in inflammatory bowel disease, acute hepatitis, and sepsis models (Oikawa *et al*, 2022). Wu *et al* (2022) reported that OTUD1 moderates intestinal inflammation by inhibiting RIPK1-mediated NF-κB activation. OTUD1 has also been reported as a potential target for the treatment of neoplastic disorders(Song *et al*, 2021). However, the role of OTUD1 in cardiovascular diseases and vascular dysfunction remains unclear.

In the present study, we investigate the role of OTUD1 in hypertensive vascular remodeling using a mouse model with Ang II infusion. We showed OTUD1 expression was up-regulated in the aortic endothelium of Ang II-induced hypertensive mice. OTUD1 deletion attenuated vascular remodeling and collagen deposition by inhibiting endothelial-to-mesenchymal transition (EndMT), whereas OTUD1 overexpression aggravated these changes both *in vivo* and *in vitro*. Mechanistically, we found that OTUD1 sustained the stability of a transcriptional factor, mothers against decapentaplegic homolog 3 (SMAD3) and facilitated SMAD3/SMAD4 complex formation through reversing the K48- and K63-linked ubiquitination of SMAD3. Collectively, we identified OTUD1 as a novel regulator of hypertensive vascular remodeling.

Results

OTUD1 is up-regulated in aortic endothelium of Ang II-induced mice

We have previously screened the mRNA levels of all deubiquitinase members in OTU family in the aortas of control and Ang II-infused mice. Among these genes, the mRNA level of *Otud1* was significantly increased in the aortas of Ang II-infused mice (Fig 1A), indicating a potential relevance of OTUD1 with vascular remodeling. We further validated the result using western blot and real-time qPCR assay. As shown in Fig 1B–D, OTUD1 was really up-regulated in the aortas of Ang II-induced mice at both the protein and mRNA levels. We then examined the cell distribution of OTUD1 in mouse aortas. Immunofluorescence staining further showed that OTUD1 colocalized with CD31, an endothelial cell marker, rather than α-SMA, a smooth muscle cell marker (Fig 1E and F). Figure 1E and F also showed that the expression of OTUD1 was markedly up-regulated in aortic endothelium of Ang II-induced mice. We also analyzed the protein levels of OTUD1 in cultured mouse primary macrophages (MPM), mouse aortic vascular smooth muscle cells (MOVAS), and HUVEC endothelial cells, respectively. As shown in Appendix Fig S1, OTUD1 was mainly expressed and could be induced by Ang II in endothelial cells. Then we identified that

OTUD1 expression indeed increased in HUVECs challenged with Ang II in a time-dependent manner (Fig 1G and H). These data indicate that OTUD1 is up-regulated in aortic endothelium of Ang II-induced mice and may be an important mediator in Ang II-induced vascular dysfunction.

OTUD1 deletion attenuates vascular remodeling and collagen deposition through inhibiting EndMT in Ang II-induced mice

To investigate the role of OTUD1 in Ang II-induced vascular injury, global OTUD1 knockout (OTUD1$^{-/-}$) mice were used and implanted with a micro-osmotic pump containing Ang II. The knockout efficiency of OTUD1$^{-/-}$ mice was verified (Appendix Fig S2A and B). Systolic blood pressure equally rose in wild-type (WT) and OTUD1$^{-/-}$ mice with Ang II infusion (Appendix Fig S2C), indicating that OTUD1 deficiency did not affect systolic blood pressure. Histological analysis of aortic wall thickness (Fig 2A and B) and Masson's trichome staining for fibrosis (Fig 2C and D) revealed that OTUD1 deletion noticeably decreased aortic wall thickness and perivascular fibrosis. This indicated that OTUD1 deletion could mitigate deleterious vascular remodeling and collagen deposition in the aortas of mice exposed to Ang II. Considering that EndMT is involved in cardiovascular diseases including hypertension-induced vascular dysfunction (Kovacic *et al*, 2019), we hypothesized that OTUD1 exacerbated vascular remodeling and collagen deposition via EndMT. Furthermore, we identified that OTUD1 deficiency constrained EndMT in the Ang II-treated mice aortas through examining the changes and levels of key proteins associated with EndMT, including VE-cadherin, Vimentin, α-SMA, Twist, and Snail (Fig 2E and F). Moreover, the mRNA level of EndMT-related genes and fibrotic factors were consistent with the above results (Fig 2G and H). Taken together, these data evidence that OTUD1 deletion attenuates vascular remodeling and collagen deposition through inhibiting EndMT in Ang II-induced mice.

OTUD1 exacerbates Ang II-induced EndMT *in vitro*

To validate the finding that OTUD1 modulates endothelial function, HUVECs challenged with Ang II was utilized. We generated OTUD1 deficiency in HUVECs by siRNA transfection (Fig 3A). OTUD1 deficiency reversed the changes of EndMT-related proteins and suppressed EndMT in HUVECs exposed to Ang II at both the protein and mRNA levels (Fig 3B and C, and Appendix Fig S3A). In addition, the mRNA levels of *Tgfb1* and *Col1a1* showed that OTUD1 deletion inhibited subsequent collagen deposition (Fig 3C). Meanwhile, OTUD1 was overexpressed in HUVECs after Flag-OTUD1 transfection (Fig 3D). OTUD1 overexpression aggravated EndMT in HUVECs challenged with Ang II at both the protein and mRNA level (Fig 3E and F, and Appendix Fig S3B). The mRNA levels of *Tgfb1* and *Col1a1* also proved that OTUD1 overexpression worsened subsequent collagen deposition (Fig 3F). To confirm the role of OTUD1 in endothelial cells, we further utilized two more vascular endothelial cell lines, bEnd.3 and EA.hy926. As expected, OTUD1 deficiency also reversed the Ang II-induced changes of EndMT-related genes in both bEnd.3 and EA.hy926 cells (Appendix Fig S4A–D). In summary, these results indicate that OTUD1 exacerbates Ang II-induced vascular remodeling and collagen deposition via EndMT in vascular endothelial cells.
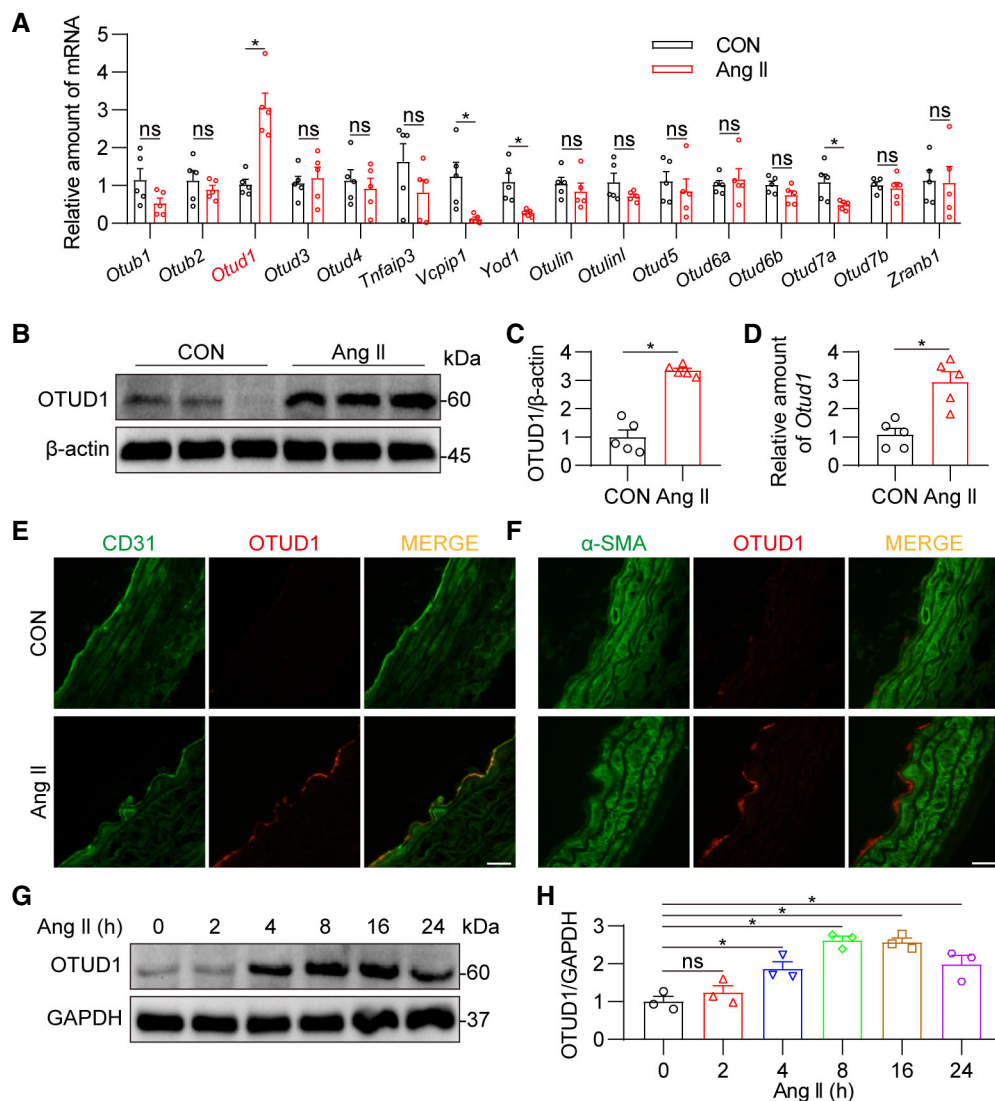
Figure 1. OTUD1 is up-regulated in aortic endothelium of Ang II-induced mice.

A mRNA levels of members of OTU family in aortas of control and Ang II-induced mice were determined by RT-qPCR. The values were normalized to *Rn18s* (*n* = 5 biological replicates).

B, C Western blot analysis (B) and densitometric quantification (C) of OTUD1 in aortas of control and Ang II-induced mice. β-Actin was used as the loading control (*n* = 5 biological replicates).

D mRNA levels of OTUD1 in aortas of control and Ang II-induced mice were determined by RT-qPCR. The values were normalized to Rn18s (*n* = 5 biological replicates).

E Representative immunofluorescence staining of CD31 (green) and OTUD1 (red) of aortic sections (scale bar = 25 μm).

F Representative immunofluorescence staining of α-SMA (green) and OTUD1 (red) of aortic sections (scale bar = 25 μm).

G, H Time-course of OTUD1 induction in response to Ang II in HUVECs. HUVECs were exposed to 1 μM Ang II for indicated time. Western blot analysis (G) and densitometric quantification (H) of OTUD1 were shown (*n* = 3 biological replicates). GAPDH was used as the loading control. Data were shown as mean ± SEM; *, *P* < 0.05; ns, not significant, two-tailed unpaired Student's *t*-test.

Source data are available online for this figure.

OTUD1 associates with the MH2 domain of SMAD3 and reverses the K48- and K63-linked ubiquitination of SMAD3 via cysteine 320 on OTUD1

To investigate the mechanism by which OTUD1 facilitates EndMT in HUVECs, we performed a LC–MS/MS analysis using HUVECs transfected with Flag-OTUD1 (Fig 4A) and, interestingly, the mass spectrometry data identified SMAD3 as a binding protein of OTUD1 (Fig 4B, and Appendix Tables S1 and S2). Besides, we also performed a RNA-sequencing using the mouse aortas tissues from WT + Ang II and KO + Ang II groups. The GSEA of transcriptome sequencing showed the effect of OTUD1 was related to the TGFβ-
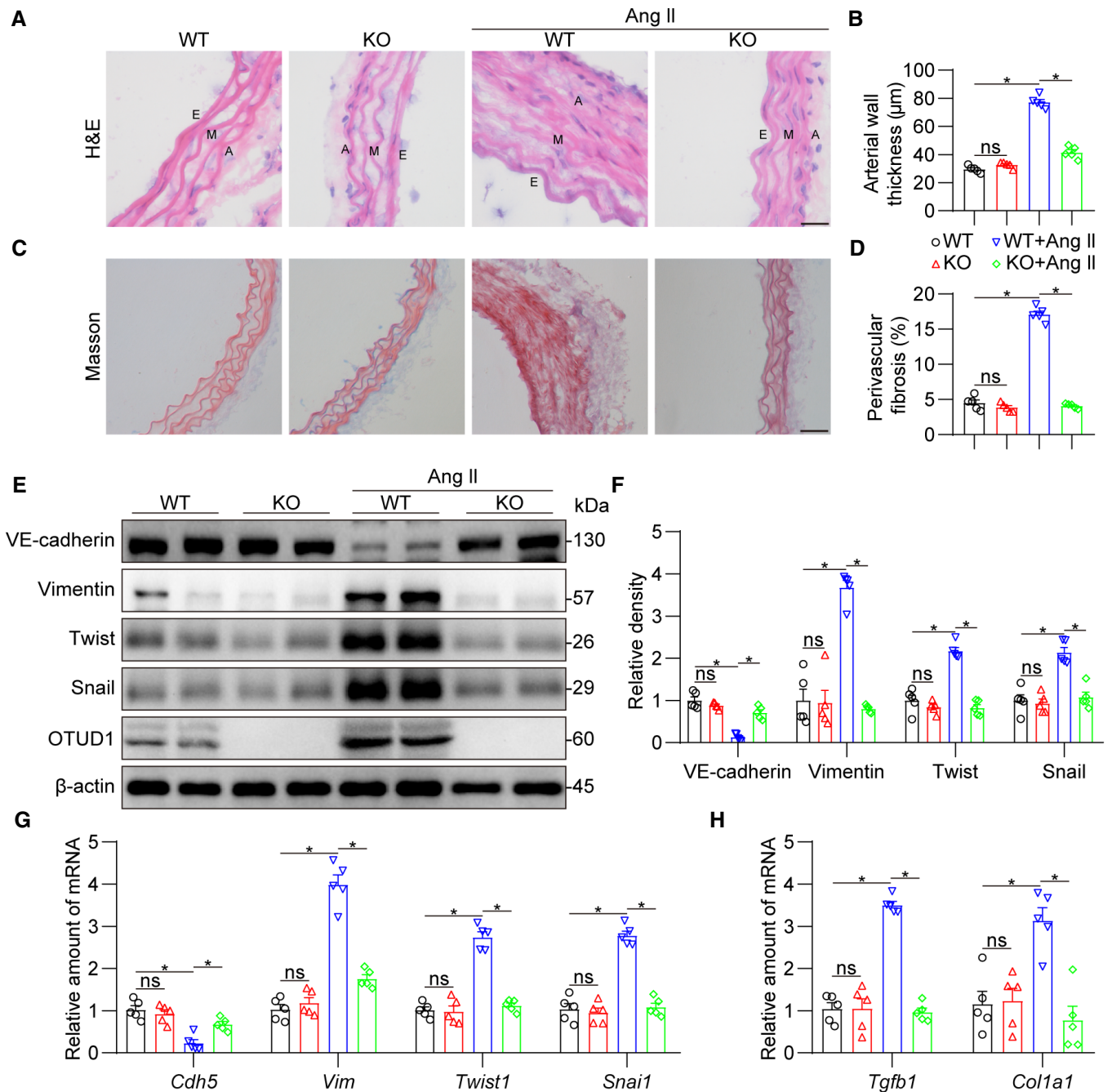
Figure 2. OTUD1 deletion attenuates vascular remodeling and collagen deposition through inhibiting EndMT in Ang II-induced mice.

A   Representative images of H&E staining of aortic sections of the mice from four groups (scale bar = 25 μm). E, endothelium; M, media; A, adventitia.

B   The quantification of arterial wall thickness in panel (A); n = 5 biological replicates.

C   Representative images of Masson's Trichrome staining of aortic sections of the mice (scale bar = 50 μm).

D   The quantification of collagen deposition in panel (C); n = 5 biological replicates.

E, F   Western blot analysis (E) of VE-cadherin, Vimentin, Twist, Snail, and OTUD1 and densitometric quantification (F) of VE-cadherin, Vimentin, Twist and Snail in aortic tissues of the mice. β-Actin was used as the loading control (n = 5 biological replicates).

G, H   mRNA levels of *Cdh5*, *Vim*, *Twist1*, *Snai1* (G), *Tgfb1* and *Col1a1* (H) in aortic tissues of the mice were examined by real-time qPCR assay. The values were normalized to Rn18s (n = 5 biological replicates). Data were shown as mean ± SEM; *, $P < 0.05$; ns, not significant, two-tailed unpaired Student's t-test.

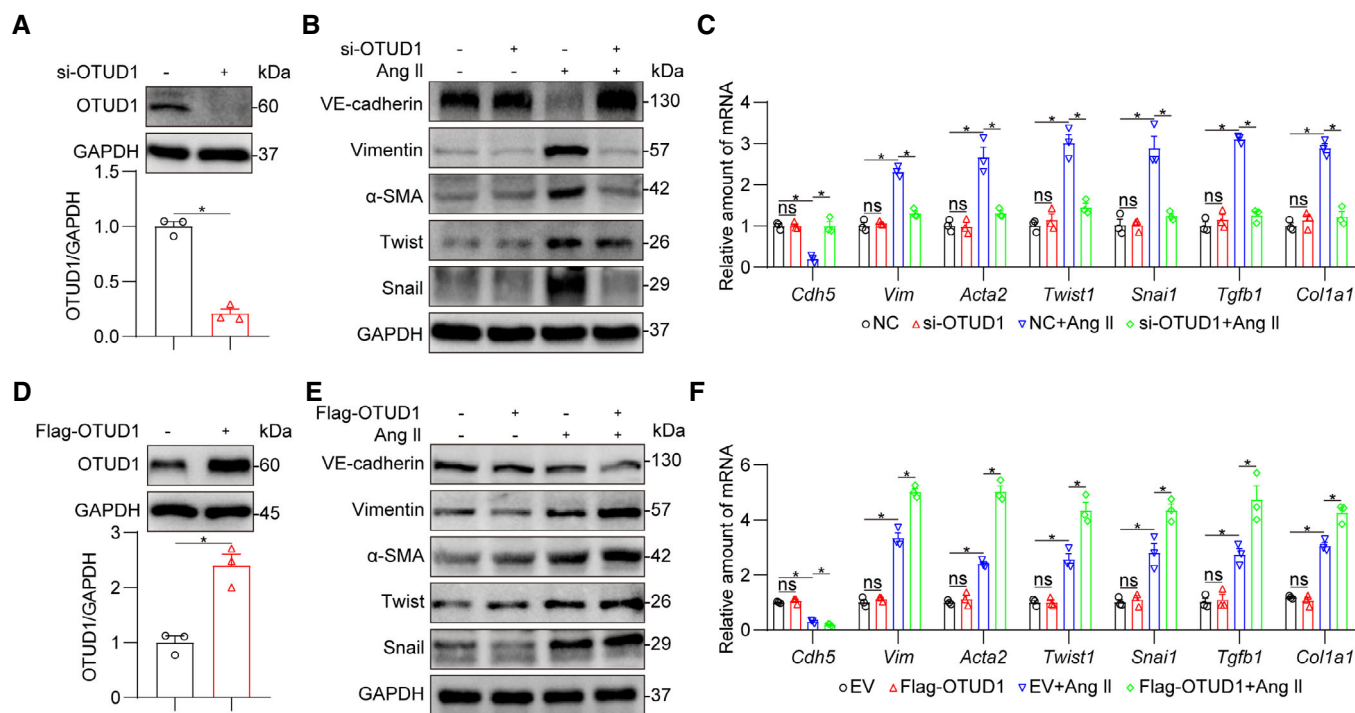Source data are available online for this figure.

Figure 3. OTUD1 exacerbates Ang II-induced EndMT in HUVECs.

A HUVECs were transfected with OTUD1 siRNA (si-OTUD1) for 24 h, while the control cells were transfected with negative control (NC) siRNA. Levels of OTUD1 protein were measured by Western blot (*n* = 3 biological replicates).

B HUVECs transfected with si-OTUD1 or NC were challenged with 1 μM Ang II for 24 h. Western blot analysis of VE-cadherin, Vimentin, α-SMA, Twist, and Snail were performed. GAPDH was used as the loading control.

C HUVECs transfected with si-OTUD1 or NC were challenged with 1 μM Ang II for 24 h. mRNA levels of *Cdh5*, *Vim*, *Acta2*, *Twist1*, *Snai1*, *Tgfb1*, and *Col1a1* were determined by RT-qPCR (*n* = 3 biological replicates). The values were normalized to β-Actin.

D HUVECs were transfected with Flag-OTUD1 plasmid for 24 h. Control cells were transfected with empty vector (EV). Levels of OTUD1 were measured by Western blot (*n* = 3 biological replicates).

E HUVECs transfected with Flag-OTUD1 or EV were challenged with 1 μM Ang II for 24 h. Western blot analysis of VE-cadherin, Vimentin, α-SMA, Twist and Snail were performed. GAPDH was used as the loading control.

F HUVECs transfected with Flag-OTUD1 or EV were challenged with 1 μM Ang II for 24 h. mRNA levels of *Cdh5*, *Vim*, *Acta2*, *Twist1*, *Snai1*, *Tgfb1*, and *Col1a1* were determined via RT-qPCR (*n* = 3 biological replicates). The values were normalized to β-actin. Data were shown as mean ± SEM; *, *P* < 0.05; ns, not significant, two-tailed unpaired Student's *t*-test.

Source data are available online for this figure.

SMAD signaling pathway (Appendix Fig S5A–C), wherein SMAD3 is an essential mediator (Derynck & Zhang, 2003) and could be ubiquitinatied (Zhang *et al*, 2014). Ang II challenge has been widely reported to be able to activate the TGFβ/SMAD3 signaling pathway (Mezzano *et al*, 2001; Rosenkranz, 2004; Schluter & Wenzel, 2008) and we also confirmed the activation of TGFβ/SMAD3 signal by Ang II in HUVECs (Appendix Fig S6). In addition, TGFβ-SMAD3 signaling pathway has been reported to be a prominent EndMT inducer (Wynn, 2008; Ma *et al*, 2020) and SMAD3 plays an essential role in Ang II-induced vascular remodeling (Sorescu, 2006). Therefore, we may hypothesize that OTUD1 regulates vascular EndMT via deubiquitinating modification of SMAD3.

Firstly, the interaction between OTUD1 and SMAD3 was determined in HUVECs using co-immunoprecipitation (Fig 4C). Interestingly, we observed that OTUD1 did not bind to SMAD2, indicating a specificity of OTUD1 towards SMAD3 (Fig 4C). The combination of OTUD1 and SMAD3 was further verified in 293T cells transfected with both Flag-OTUD1 and HA-SMAD3 plasmids (Fig 4D). We also

confirmed that endogenous OTUD1 could interact with SMAD3 in HUVECs challenged with Ang II (Appendix Fig S7). Next, we examined the nature of the interaction between OTUD1 and SMAD3. SMAD3 protein consists of three domains including MH1, Linker, MH2 (Derynck & Zhang, 2003; Fig 4E). As shown in Fig 4F, OTUD1 coupled with SMAD3, SMAD3$^{\Delta MH1}$ and SMAD3$^{\Delta Linker}$, rather than SMAD3$^{\Delta MH2}$, suggesting that OTUD1 bound to MH2 domain of SMAD3. By the way, although a previous study reported that OTUD1 deubiquitinates SMAD7 via a K33-linked manner in breast cancer cells (Zhang *et al*, 2017), we did not find SMAD7 as OTUD1-binding protein in our LC–MS/MS analysis. We also excluded the OTUD1-SMAD7 interaction in HUVECs using the co-immunoprecipitation assay (Appendix Fig S8).

We then determined that OTUD1 could deubiquitinate SMAD3 in 293T cells (Fig 4G). Cysteine at position 320 in OTUD1 has been identified as an active site for the deubiquitinating activity (Yao *et al*, 2018). We mutated cysteine 320 to serine and found that OTUD1 mutant (C320S) could no longer remove ubiquitin molecules

from SMAD3 (Fig 4H), manifesting that the ability of OTUD1 to deubiquitinate SMAD3 depends on the catalytic site C320. SMAD3 has been reported to be modified by different forms of ubiquitination (Herhaus *et al*, 2013; Liu *et al*, 2022). The K48- and K63-linked ubiquitination are most classic types in ubiquitinating modification. We further determine which type of ubiquitin chain on SMAD3 was deubiquitinated by OTUD1. As shown in Fig 4I, OTUD1 decreased both K48- and K63-linked polyubiquitin chains of SMAD3, indicating that OTUD1 reverses both K48- and K63-linked ubiquitination of

SMAD3. Although OTUD1 induces K33-linked deubiquitination of SMAD7 (Zhang *et al*, 2017), we found that OTUD1 failed to remove K33-linked ubiquitin chains from SMAD3 (Appendix Fig S9).

OTUD1 sustains SMAD3 stability and facilitates SMAD3/SMAD4 complex formation

The K48-linked ubiquitin chain is a prominent linkage and proteins modified with such ubiquitin chains are often degraded by the 26 S
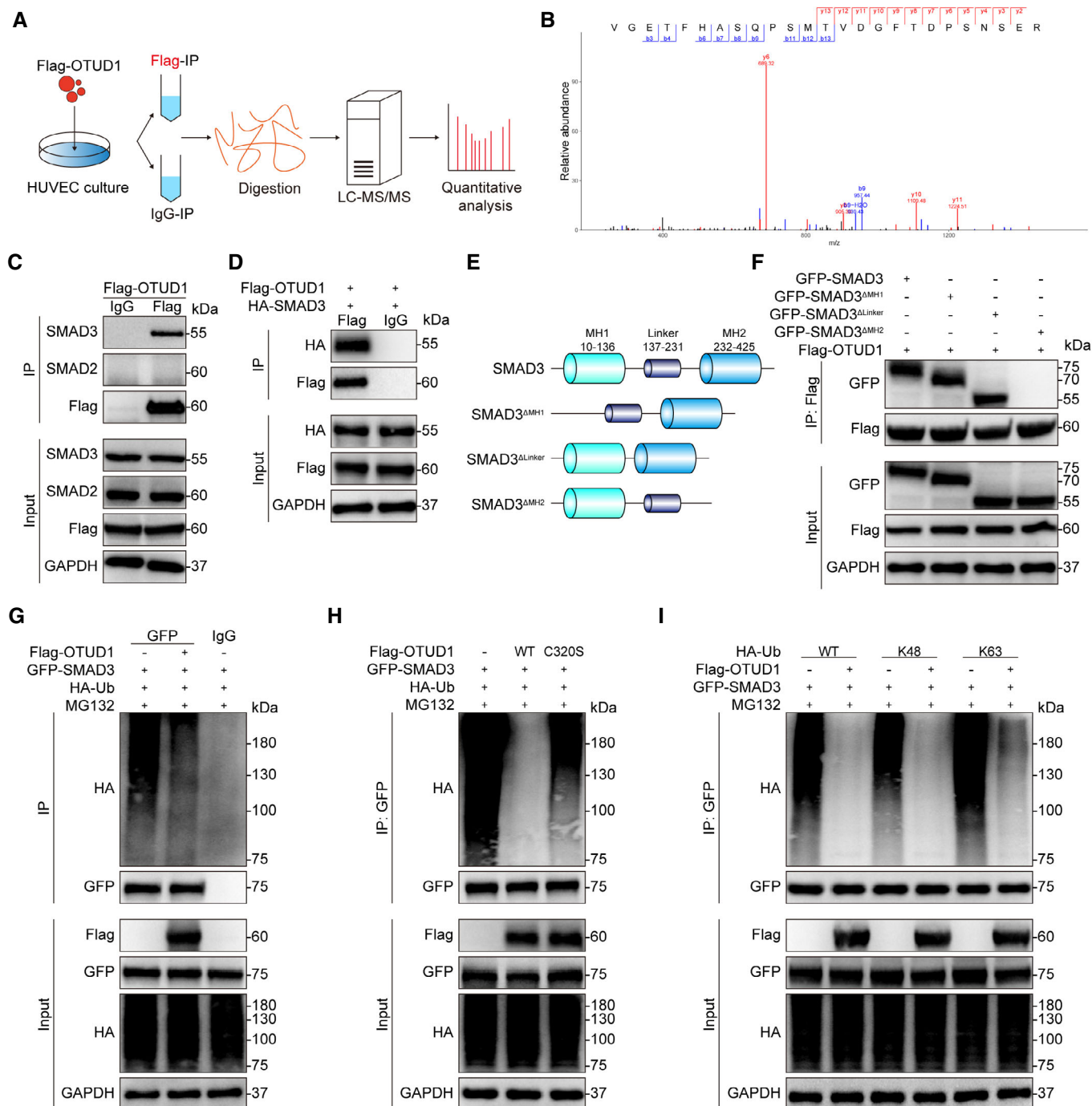

Figure 4.

Figure 4. OTUD1 associates with the MH2 domain of SMAD3 and reverses the K48- and K63-linked ubiquitination of SMAD3 via cysteine 320 on OTUD1.

A   Schematic illustration of quantitative proteomic screen to identify proteins binding to OTUD1.
B   MS/MS spectrum of the peptide showing TVDGFTDPSNSER from SMAD3.
C   Co-immunoprecipitation of OTUD1 and SMAD2 or SMAD3 in HUVECs transfected with Flag-OTUD1. Exogenous Flag-OTUD1 was immunoprecipitated by anti-Flag antibody. IgG, immunoglobulin G.
D   Co-immunoprecipitation of OTUD1 and SMAD3 in 293T cells co-transfected with Flag-OTUD1 and HA-SMAD3. OTUD1 and SMAD3 were immunoprecipitated by anti-Flag and anti-HA antibodies, respectively. IgG, immunoglobulin G.
E   The protein structure of SMAD3 and the schematic illustration of SMAD3 domain deletion constructs.
F   Identification of the OTUD1-binding domain of SMAD3. Plasmids encoding GFP-labeled SMAD3, or three GFP-labeled SMAD3 mutants (mut-SMAD3), respectively, and Flag-OTUD1 were transfected in 293T cells for 24 h. The interactions between OTUD1 and SMAD3 or SMAD3 mutants were determined by co-immunoprecipitation using anti-Flag and anti-GFP antibodies.
G   Immunoprecipitation of SMAD3 in 293T cells co-transfected with GFP-SMAD3, HA-Ub and Flag-OTUD1 and then challenged with 10 μM MG132 for 6 h. Ubiquitinated SMAD3 was detected by immunoblotting using anti-HA antibody.
H   Immunoprecipitation of SMAD3 in 293T cells co-transfected with GFP-SMAD3, HA-Ub, and Flag-OTUD1 or Flag-OTUD1(C320S), and then challenged with 10 μM MG132 for 6 h. Ubiquitinated SMAD3 was detected by immunoblotting using anti-HA antibody.
I   Immunoprecipitation of SMAD3 in 293T cells co-transfected with GFP-SMAD3, Flag-OTUD1, and HA-Ub, HA-Ub-K48 (K48 only), or HA-Ub-K63 (K63 only), respectively, and then challenged with 10 μM MG132 for 6 h. Ubiquitinated SMAD3 was detected by immunoblotting using anti-HA antibody.

Source data are available online for this figure.

proteasome (Komander & Rape, 2012). Thus, we explored whether OTUD1 could maintain SMAD3 stability and protect it from proteasomal degradation. As expected, OTUD1 overexpression increased SMAD3 protein level in a dose-dependent manner (Fig 5A and B), while the mRNA level of SMAD3 was not affected (Appendix Fig S10). CHX pulse-chase assay was performed to reveal that OTUD1 obviously prevented SMAD3 from proteasomal degradation (Fig 5C and D). Moreover, we confirmed that the level of SMAD3 protein in the aortas of OTUD1$^{-/-}$ mice was significantly lower than that in the aortas of WT mice (Fig 5E and F), which is consistent with the *in vitro* results.

On the other side, K63-linked chains are mainly considered as nondegradative ubiquitin chains that modulate protein enzyme activity, nuclear translocation, or interaction with other proteins (Xu *et al*, 2009). Given that OTUD1 also regulates K63-linked ubiquitination of SMAD3, we examined the potential effect of OTUD1 on SMAD3 behaviors, including phosphorylation, translocation, and SMAD3-SMAD4 interaction. Surprisingly, OTUD1 did not affect the phosphorylation level of SMAD3 (Appendix Fig S11A). Activated SMAD3 forms a complex with SMAD4 and then translocates into the nucleus to regulate target gene expression (Derynck & Zhang, 2003). We then examined if OTUD1 may promote SMAD3/SMAD4 complex formation through removing the K63-linked polyubiquitin chain of SMAD3. Indeed, we observed that either total ubiquitination or K63-linked ubiquitination of SMAD3 could inhibit the interaction between SMAD3 and SMAD4 (Fig 5G). Then, the co-immunoprecipitation assay revealed that OTUD1 could promote SMAD3/SMAD4 complex formation, through deubiquitination modification of SMAD3 (Fig 5H). SMAD3-SMAD4 interaction promotes the nuclear translocation of this complex to regulating target gene expression. As expected, OTUD1 deletion suppressed Ang II-induced SMAD3 nuclear translocation in HUVECs (Fig 5I).

Next, we explored the role of SMAD3 in mediating the actions of OTUD1. We transfected HUVECs with OTUD1 plasmid to express OTUD1 and then challenged the cells with Ang II in the presence or absence of SMAD3 inhibitor. We used a small-molecule inhibitor SIS3, which selectively inhibits SMAD3 (Jinnin *et al*, 2006). In our experiments, SMAD3/SMAD4 complex formation and SMAD3 nuclear translocation induced by OTUD1 were significantly reversed by SIS3 (Appendix Fig S11B and C). Also, SMAD3 knockdown reduced mRNA levels of EndMT-related and pro-fibrotic genes in

HUVECs upon Ang II exposure, even in the presence of OTUD1 expression (Appendix Fig S11D and Fig 5J and K). These *in vitro* studies show that OTUD1 interacts with SMAD3 and regulates SMAD3 stability and facilitates SMAD3/SMAD4 complex formation to module expression of EndMT-related genes.

OTUD1 overexpression aggravates vascular remodeling and collagen deposition through regulating SMAD3 in mice

Finally, we planned to examine if SMAD3 mediates OTUD1-promoted vascular remodeling in mice. To achieve this goal, we constructed AAV9-encoding OTUD1 particles and administered them to mice via tail vein injection. AAV9 infection was successful and showed increased OTUD1 expression in the aortas of mice (Appendix Fig S12A and B). We also treated some mice with SMAD3 inhibitor SIS3. Mice were then infused with saline or Ang II for 2 weeks. Ang II-increased systolic blood pressure in mice was not affected by either OTUD1 overexpression or SMAD3 inhibitor SIS3 (Appendix Fig S12C). Histological analysis of aortic wall thickness (Fig 6A and B) and Masson's trichome staining for fibrosis (Fig 6C and D) revealed that OTUD1 overexpression increased aortic wall thickness and perivascular fibrosis, while SIS3 treatment abolished the deterioration of aortas caused by OTUD1 overexpression and Ang II infusion. OTUD1 overexpression resulted in more severe EndMT in the aortas, as evidenced by the change profile of EndMT-related proteins, whereas SIS3 offset the changes of OTUD1 (Fig 6E and F). In addition, it was observed that OTUD1 overexpression by AAV9-OTUD1 increased the protein level of SMAD3 in mouse aortas (Fig 6E and F). Similar results were observed at the mRNA levels of these EndMT-related genes (Fig 6G). As expected, the mRNA levels of fibrotic factors were consistent with the above results (Fig 6H). These data demonstrate that OTUD1 overexpression exasperated deleterious vascular remodeling and collagen deposition in the aortas through regulating SMAD3.

Discussion

In this study, we evaluated the role of OTUD1 in Ang II-induced vascular remodeling both *in vivo* and *in vitro*. The three key findings
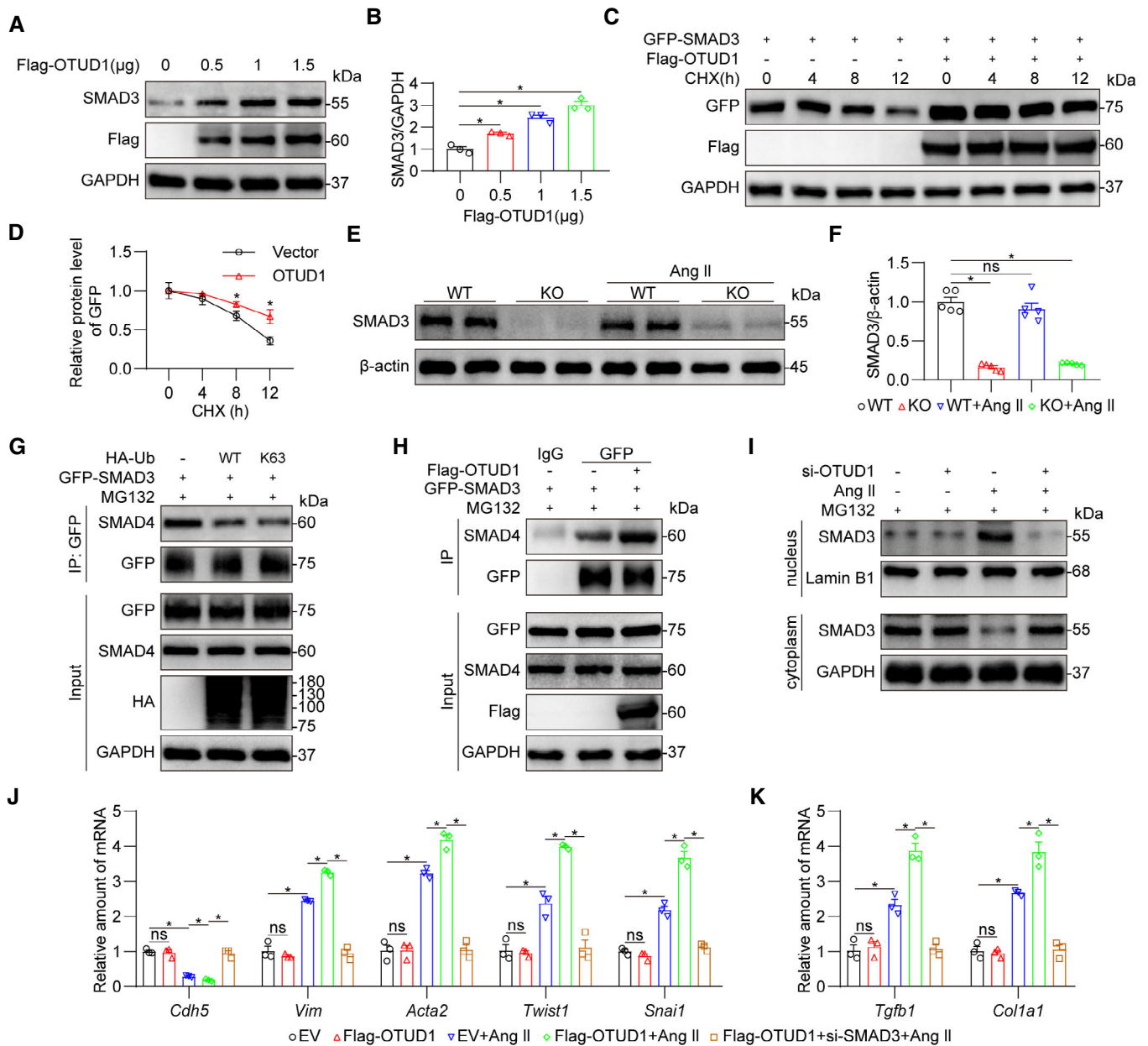
Figure 5. OTUD1 sustains SMAD3 stability and facilitates SMAD3/SMAD4 complex formation and nuclear translocation.

A, B   293T cells were transfected with various amount of Flag-OTUD1. Western blot analysis (A) and densitometric quantification (B) of SMAD3. GAPDH was used as the loading control ($n = 3$ biological replicates).

C, D   293T cells transfected with GFP-SMAD3 and Flag-OTUD1 were treated with cycloheximide (CHX, 50 μg/ml) at the indicated time points. Western blot analysis (C) and densitometric quantification (D) of GFP are shown. GAPDH was used as the loading control ($n = 3$ biological replicates).

E, F   Western blot analysis (E) and densitometric quantification (F) of SMAD3 in aortic tissues of the mice from four groups. β-Actin was used as the loading control ($n = 5$ biological replicates).

G   Co-immunoprecipitation of SMAD3 and SMAD4 in 293T cells co-transfected with GFP-SMAD3, HA-Ub, and HA-Ub-K63 (K63 only), respectively, and then challenged with 10 μM MG132 for 6 h. Exogenous SMAD3 was immunoprecipitated by anti-GFP antibody.

H   Co-immunoprecipitation of SMAD3 and SMAD4 in 293T cells co-transfected with GFP-SMAD3 and Flag-OTUD1 and then challenged with 10 μM MG132 for 6 h. Exogenous SMAD3 was immunoprecipitated by anti-GFP antibody. IgG, immunoglobulin G.

I   HUVECs transfected with OTUD1 siRNA or NC siRNA were challenged with 1 μM Ang II for 24 h and with 10 μM MG132 6 h before harvest. Protein levels of SMAD3 in cytoplasm and nucleus were measured by Western blot assay. GAPDH was used as the loading control for cytosolic fractions. Lamin B1 was used as the loading control for nuclear fractions.

J, K   HUVECs transfected with Flag-OTUD1 (or EV) and si-SMAD3 were challenged with 1 μM Ang II for 24 h. mRNA levels of *Cdh5, Vim, Acta2, Twist1, Snai1* (J), *Tgfb1 and Col1a1* (K) were determined by RT-qPCR assay ($n = 3$ biological replicates). The values were normalized to those of β-Actin. Data were shown as mean ± SEM; *, $P < 0.05$; ns, not significant, two-tailed unpaired Student's *t*-test.

Source data are available online for this figure.

are the following: (i) OTUD1 promotes Ang II-induced vascular remodeling and collagen deposition through exacerbating EndMT. (ii) OTUD1 associates with the MH2 domain of SMAD3 and reverses the K48- and K63-linked ubiquitination of SMAD3 in endothelial cells. (iii) OTUD1 sustains SMAD3 stability and facilitates SMAD3/SMAD4 complex formation to regulate the transcription of genes involved in vascular EndMT and remodeling. A schematic representation of the main findings is presented in the graphical abstract.
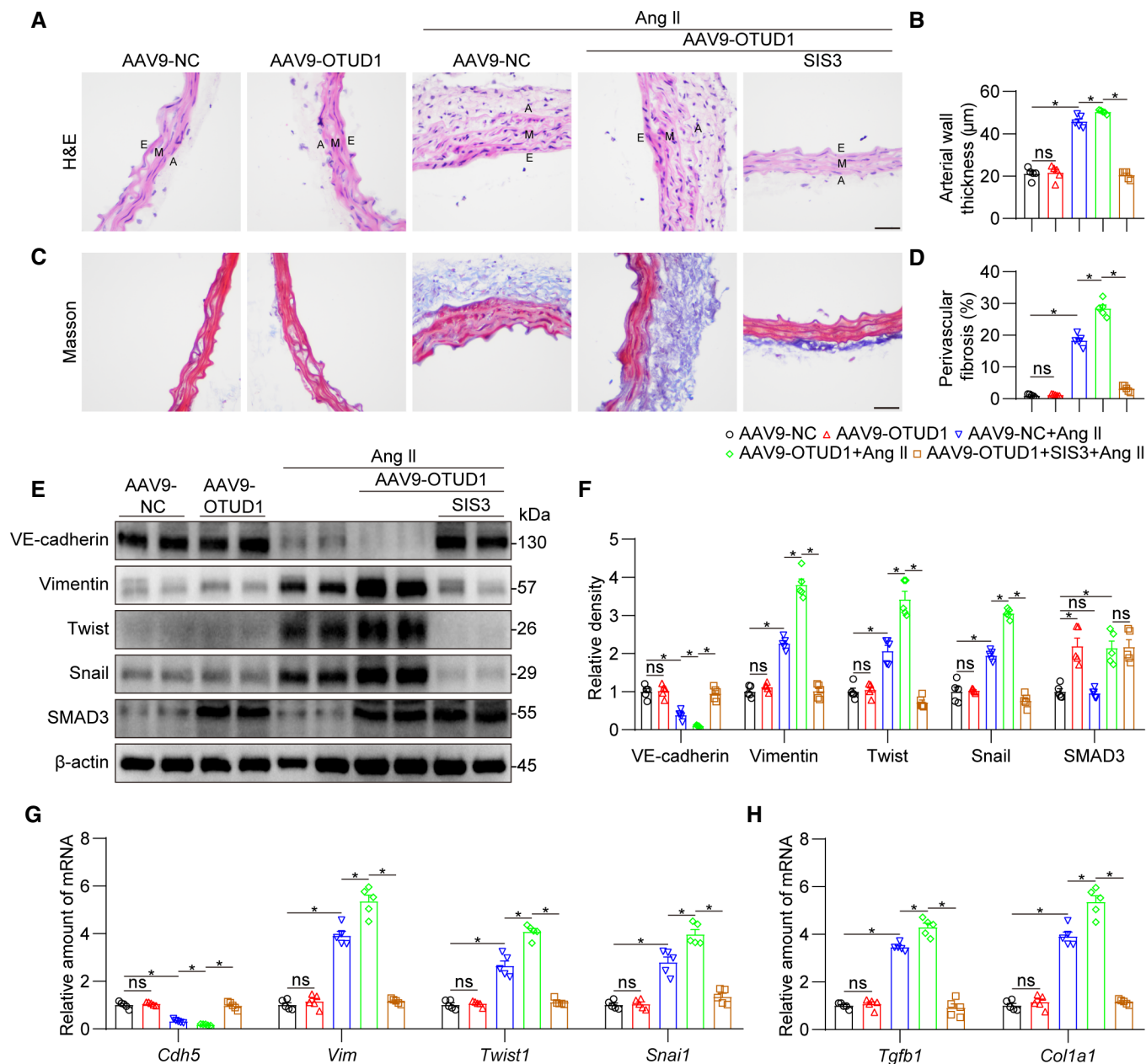

Figure 6. OTUD1 overexpression aggravates vascular remodeling and collagen deposition through regulating SMAD3 *in vivo*.
The methodology of this animal experiment was described in Materials and Methods.
A, B   Representative images (A) of H&E staining of aortic sections (scale bar = 25 μm) and quantification of arterial wall thickness (B); $n = 5$ biological replicates. E, endothelium; M, media; A, adventitia.
C–H   Representative images (C) of Masson's Trichrome staining of aortic sections (scale bar = 25 μm) and quantification of collagen deposition (D); $n = 5$ biological replicates. Western blot analysis (E) and densitometric quantification (F) of VE-cadherin, Vimentin, Twist and Snail in aortic tissues. β-Actin was used as the loading control ($n = 5$ biological replicates). mRNA levels of *Cdh5*, *Vim*, *Twist1*, *Snai1* (G), *Tgfb1* and *Col1a1* (H) in aortic tissues were examined by real-time qPCR. The values were normalized to Rn18s ($n = 5$ biological replicates). Data were shown as mean ± SEM; *, $P < 0.05$; ns, not significant, two-tailed unpaired Student's *t*-test.

Source data are available online for this figure.

Vascular endothelial cells can obtain a mesenchymal phenotype upon irritation or injury in a process termed EndMT (Chen *et al*, 2015). EndMT is an intricate cellular differentiation process in which endothelial cells lose endothelial markers such as VE-cadherin and acquire mesenchymal features such as α-SMA, vimentin and fibrotic markers (Bischoff, 2019). And increased expression of EndMT transcription factors including Snail and Twist1 indicates EndMT. As EndMT evolves, cells migrate and contribute to extensive vascular remodeling (Piera-Velazquez & Jimenez, 2019). Previous studies have identified that EndMT is involved in Ang II-induced vascular remodeling (Li *et al*, 2020; Lin *et al*, 2020; Qian *et al*, 2021). The TGFβ-SMAD3 signaling pathway is a primary EndMT inducer (Pardali *et al*, 2017; Bischoff, 2019; Ma *et al*, 2020). Activated SMAD3 combines with SMAD4 and translocates into the nucleus where the SMAD3/SMAD4 complex regulates the transcription of EndMT-associated proteins (Derynck & Zhang, 2003; Meng *et al*, 2016). Li *et al* (2010) reported that inhibition of SMAD3 with the inhibitor SIS3 restrained EndMT and delayed the progression of diabetic nephropathy. SMAD3-specific gene deletion in the liver prevented hepatocytic EndMT (Ju *et al*, 2006). In our study, OTUD1 promoted Ang II-induced vascular remodeling and collagen deposition through inhibiting EndMT. Moreover, we demonstrated that OTUD1 bound to the MH2 domain of SMAD3 to sustain SMAD3 stability and facilitate SMAD3/SMAD4 complex formation, thus boosting the transcriptional activity of SMAD3 in endothelial cells.

DUBs are crucial components in pathological vascular remodeling (Wang *et al*, 2020). Xia *et al* (2021) reported that USP10 participates in vascular remodeling by promoting VSMC proliferation and migration via stabilizing Skp2 protein expression. And Ioannis *et al* showed that WNT5A regulated vascular redox signaling via USP17 in obesity (Akoumianakis *et al*, 2019). Besides, Gao *et al* (2010) demonstrated that CYLD mediates vascular endothelial cell migration via Rac1 activation. Nevertheless, it is unclear whether OTUD1 is involved in vascular remodeling and other cardiovascular diseases. This study for the first time identified OTUD1 as an indispensable mediator in Ang II-induced vascular remodeling. Most importantly, we have elucidated that OTUD1 expedited vascular remodeling by deubiquitinating SMAD3. Therefore, OTUD1 may be a potential target for treating hypertensive vascular remodeling.

The SMAD3 transcription factor lies at the core of the TGFβ signaling pathway (Massague *et al*, 2005). Phosphorylated SMAD3 forms a complex with SMAD4 and translocates into the nucleus where it regulates the transcription of target genes (Derynck & Zhang, 2003). SMAD3 is involved in Ang II-induced vascular remodeling (Sorescu, 2006; Wang *et al*, 2006). Previous studies have shown that SMAD3 can be ubiquitinated (Izzi & Attisano, 2004; Inoue & Imamura, 2008). Meanwhile, some studies showed that multiple DUBs could regulate the deubiquitination of SMAD3. OTUB1 and UCHL5 stabilize SMAD3 by reversing the ubiquitination of SMAD3 (Herhaus *et al*, 2013; Nan *et al*, 2016). Moreover, USP15 enhances SMAD3/SMAD4 complex formation by deubiquitinating SMAD3 (Xie *et al*, 2014). Huang *et al* (2021) reported that USP7 facilitates SMAD3 expression and the DNA-binding of the SMAD3-SMAD4 dimer at the SMAD3 locus to repress lung cancer. So far, there is no DUBs reported to deubiquitinate SMAD3 in K63-linked way and regulate SMAD3 phosphorylation. Here, we identified

OTUD1 as a new DUB regulating SMAD3 by binding to the MH2 domain of SMAD3. Interestingly, we found that OTUD1 regulates SMAD3 through two ways. On the one hand, OTUD1 sustained SMAD3 stability via reversing K48-linked ubiquitin chains. On the other hand, OTUD1 assisted SMAD3/SMAD4 complex formation by catalyzing the deubiquitination of K63-linked SMAD3. Although the involved lysine residues in SMAD3 are not identified, to the best of our knowledge, this is the first study to see that SMAD3 is able to deubiquitinated simultaneously in both K48- and K63-linked ways by a DUB. This study provides a new post-transcriptional modification of SMAD3 regulation.

It is undeniable that this study has some limitations. We used the global OTUD1 knockout (OTUD1$^{-/-}$) mice to investigate the role of OTUD1 in Ang II-induced vascular remodeling. We showed that OTUD1 expression was much less in macrophages and smooth muscles cells, compared with that in endothelial cells. Our *in vitro* experiments using three endothelial cell lines validate the role OTUD1 in endothelial cells. We also showed that overexpression of OTUD1 in blood vessels via AAV9 infection significantly enhanced Ang II-induced vascular remodeling. Thus, the current data from both *in vitro* and *in vivo* experiments should be able to support our conclusion. However, we acknowledge that the utilization of endothelial cell-specific OTUD1 knockout mice may strengthen this conclusion. It is imperative for future studies to utilize endothelial cell-specific OTUD1 knockout mice to rule out the effects of OTUD1 in other cell types. In addition, the specific lysine residues of SMAD3 involved in the ubiquitination regulation of OTUD1 were not determined. This is a major aspect that future research should clarify. Finally, our study focuses on the OTUD1-SMAD3 axle in mediating Ang II-induced EndMT. It is unclear how Ang II induces OTUD1 overexpression in mouse aortas and cultured HUVECs, which is an important problem that future research.

In conclusion, the current study identified upregulated OTUD1 in the vascular endothelium of Ang II-challenged mice and showed that Ang II-induced vascular remodeling and fibrosis are essentially prevented when OTUD1 is knocked out. Conversely, increased expression of OTUD1 enhances Ang II-induced vascular injuries in both mice and cultured HUVECs. Mechanistically, we identified SMAD3 as an important OTUD1 substrate. OTUD1 stabilizes SMAD3 and facilitates SMAD3/SMAD4 complex formation and subsequent nuclear translocation through both K48- and K63-linked deubiquitination. To our knowledge, this is the first study to demonstrate that endothelial OTUD1 promoted Ang II-induced vascular remodeling by deubiquitinating SMAD3. This finding extends our understanding of the effect of DUBs on Ang II-induced vascular remodeling and indicates that OTUD1 is a potential therapeutic target for vascular remodeling-related diseases.

Materials and Methods

Reagents

Angiotensin II (Ang II, Cat. No: HY-13948) was purchased from MedChemExpress (New Jersey, USA). Small interfering RNAs were purchased from RiboBio (Guangzhou, China). Plasmids (Flag-OTUD1, Flag-OTUD1 (C320S), HA-SMAD3, GFP-SMAD3, GFP-mut-SMAD3, HA-Ub, HA-Ub-K33, HA-Ub-K48 and HA-Ub-K63) and

AAV9 (OTUD1 and negative control) were obtained from Genechem (Shanghai, China). Antibodies against GAPDH (#5174), β-actin (#3700), p-SMAD3 (#9520), SMAD3 (#9523) and SMAD2 (#5339) were purchased from Cell Signaling Technology (Danvers, MA, USA). Antibodies against VE-cadherin (#ab33168), Vimentin (#ab8978), α-SMA (#ab7817), Twist (#ab50887), Snail (#ab216347), CD31 (#ab9498), SMAD7 (#ab216428), and Lamin B (#ab133741) were purchased from Abcam (Cambridge, UK). Antibodies against VE-cadherin (#66804-1-Ig), Twist (#25465-1-AP), Snail (#13099-1-AP), TGF-β1 (#21898-1-AP), Flag (#20543-1-AP) and HA (#51064-2-AP), GFP (#66002-1-Ig), and SMAD4 (#10231-1-AP) were purchased from Proteintech (Wuhan, China).

Animal experiments

All animal care and experimental procedures were approved by the Wenzhou Medical University Animal Policy and Welfare Committee (Approval ID: wydw2021-0057). All animal studies followed the Guide for the Care and Use of Laboratory Animals (National Institutes of Health, USA). Male C57BL/6 wild-type (WT) mice and male OTUD1 knockout (OTUD1$^{-/-}$) mice (Song et al, 2021; Wu et al, 2022) on a C57BL/6 background were obtained from Gempharmatech (Nanjing, China). The viability and proper development of OTUD1$^{-/-}$ mice were normal during the experiments. Animals were housed with a 12:12 h light–dark cycle at a constant room temperature and fed a standard rodent diet. The animals were acclimatized to the laboratory for at least 2 weeks before initiating the studies. All animal experiments were performed and analyzed by blinded experimenters. Treatment groups were assigned in a randomized fashion.

Ang II-induced hypertensive vascular remodeling in mice was performed as described previously (Guo et al, 2019). In brief, 8-week-old male mice (including WT and OTUD1$^{-/-}$ mice) were administered with subcutaneous infusions of Ang II at a dose of 1,000 ng/kg/min or saline in osmotic minipumps (Alzet MODEL 1004, CA, USA) for 4 weeks. Systolic blood pressure was measured weekly with a tail-cuff using a telemetric blood pressure system (BP-2010A, Softron Biotechnology, Tokyo, Japan). All mice were euthanized under sodium pentobarbital anesthesia and blood samples were collected. The aortas were fixed in 4% paraformaldehyde or snap-frozen in liquid nitrogen.

To overexpress OTUD1 in aortas, we infected the mice with adeno-associated virus serotype 9 (AAV9) that encodes OTUD1 (AAV9-OTUD1). Mice were injected with AAV9-OTUD1 via tail vein (3×10^{11} viral particles/mouse) for 2 weeks, followed by 2 weeks of Ang II infusion and SMAD3 inhibitor SIS3 (Jinnin et al, 2006) treatment. The control groups received the same volume of AAV9 vehicle expressing negative control sequence (AAV9-NC). SIS3 (#S0447, Sigma, St. Louis, MO, USA) was dissolved in 0.5% DMSO and mice were treated with 5 mg/kg/day by intraperitoneal injection, as previously reported (Yegodayev et al, 2020). The blood pressure measurement, anesthesia, killing, and tissue collection were performed as described above.

Histological analysis

The aorta tissues were fixed with 4% formaldehyde, dehydrated, made transparent and embedded in paraffin. The tissues were cut into 6 μm-thick sections for subsequent experiments. The slices were stained with hematoxylin and eosin (H&E, G1120, Solarbio, Beijing, China) and Masson's trichrome staining (G1340, Solarbio) according to the manufacturer's instructions.

Frozen sections were used for immunofluorescence staining. Slides were fixed in cold methanol and permeabilized using 0.5% Triton-X. Then, slides were blocked using 5% bovine serum albumin for 30 min and incubated overnight with primary antibodies. Alexa-488 and Alexa-647 conjugated secondary antibodies (Abcam, 1:200) were used for detection. The images were captured using a fluorescence microscope (Nikon, Tokyo, Japan).

Cell culture

Mouse primary peritoneal macrophages (MPMs) were isolated as described previously (Huang et al, 2022). Human umbilical vein endothelial cells (HUVECs), mouse aortic vascular smooth muscle cells (MOVAS), endothelial cell lines bEnd.3 and EA.hy926, and 293T cells were obtained from the Shanghai Institute of Biochemistry and Cell Biology (Shanghai, China) and cultured in high-glucose Dulbecco's modified Eagle's medium (DMEM; Gibco, Eggenstein, Germany) with 10% FBS and 1% penicillin/streptomycin. All cells were incubated in a humidified incubator at 37°C and 5% CO_2.

Gene knockdown and overexpression

Gene silencing and overexpression in cells were achieved by transfecting specific siRNAs and plasmids. Custom siRNAs were synthesized for human OTUD1 (5'-GCCAAAUCUAUGGCCAUAUUU-3'), mouse OTUD1 (5'-CAGAUGCUGAAUGUGAAUAUACTT-3'), and human SMAD3 (5'-GCCUGGUCAAGAAACUCAAUU-3'). Plasmids encoding Flag-OTUD1, Flag-OTUD1 (C320S), HA-SMAD3, GFP-SMAD3, GFP-mut-SMAD3, HA-Ub, HA-Ub-K48, and HA-Ub-K63 were constructed by Genechem. Transfection of HUVECs and 293T cells with siRNAs and plasmids was performed using Lipofectamine™ 3000 (Thermo Fisher Scientific, Carlsbad, CA, USA).

Western blotting and co-immunoprecipitation

Total protein from cells and aortic tissues was extracted using lysis buffer (AR0103, Boster Biological Technology, Pleasanton, CA, USA). Proteins were separated using 10% sodium dodecyl sulfate-polyacrylamide gel electrophoresis (SDS–PAGE) and transferred to polyvinylidene fluoride membranes. Before adding specific primary antibodies, the membranes were blocked in Tris-buffered saline for 1.5 h at room temperature. Protein bands were detected by incubation with horseradish peroxidase-conjugated secondary antibodies and an enhanced chemiluminescence reagent (Bio-Rad, Hercules, CA, USA). Band densities were quantified using ImageJ software (version 1.38 e, NIH, Bethesda, MD, USA) and normalized to loading controls.

For co-immunoprecipitation assays, cell extracts prepared following treatments were incubated with indicated antibodies at 4°C overnight. Then the proteins were immunoprecipitated with Protein A + G Agarose (P2012, Beyotime, Shanghai, China) at 4°C for 2 h. Immunoprecipitation samples were immunoblotted for co-precipitated protein detection. Total lysates were subjected to

western blotting analysis as input controls. Protein interactions were quantified using ImageJ software.

Real-time quantitative PCR

Total RNA was extracted from cells or aortic tissues using RNAiso Plus (9109, Takara, Shiga, Japan). Reverse transcription was performed using PrimeScript™ RT Reagent Kit with gDNA Eraser (RR047A, Takara). Quantitative PCR was performed using TB Green® Premix Ex Taq™ II (RR820A, Takara) in a QuantStudio™ 3 Real-Time PCR System (Thermo Fisher Scientific). Primers were obtained from Thermo Fisher Scientific. Primer sequences used in this study are listed in Appendix Table S3.

Transcriptome sequencing

Total RNA from aortic tissues was collected using RNAiso Plus and subjected to genome-wide transcriptomic analysis by LC-Bio (Hangzhou, China). The differentially expressed genes (DEGs) were selected with fold change > 2 or fold change < 0.5 and P-value < 0.05. Gene-set enrichment analysis (GSEA, https://www.gsea-msigdb.org/gsea/index.jsp) of the signaling pathways was performed as described by LC-Bio (https://www.lc-bio.cn/).

LC–MS/MS analysis

Anti-Flag antibody was added to the lysate of HUVECs transfected with Flag-OTUD1 for co-immunoprecipitation and IgG was used as a negative control. LC–MS/MS analysis was carried out by PTM Bio Co., Ltd. (Zhejiang, China). We screened out the substrate proteins that may bind to OTUD1 according to the score and Flag/IgG ratio of the detected proteins in the mass spectrometry data.

Statistical analysis

All experiments were randomized and blinded. Data represented at least three independent experiments and were expressed as mean ± standard error of the mean (SEM). Statistical analyses were performed with GraphPad Prism 8.0 software (GraphPad, San Diego, CA, USA). Comparisons between two groups were analyzed using Student's t-test. One-way ANOVA followed by Dunnett's *post hoc* test was used to compare more than two data groups. Statistical significance was set at $P < 0.05$. Post-tests were run only if F achieved $P < 0.05$ and there was no significant variance in homogeneity.

Data availability

The datasets produced in this study are available in the following databases:

- RNA sequencing data: Gene Expression Omnibus GSE217304 (https://www.ncbi.nlm.nih.gov/geo/).
- LC–MS/MS data: PRIDE PXD037926 (https://www.ebi.ac.uk/pride/archive).

Expanded View for this article is available online.

Disclosure and competing interests statement

The authors declare that they have no conflict of interest.

References

Akoumianakis I, Sanna F, Margaritis M, Badi I, Akawi N, Herdman L, Coutinho P, Fagan H, Antonopoulos AS, Oikonomou EK *et al* (2019) Adipose tissue-derived WNT5A regulates vascular redox signaling in obesity via USP17/RAC1-mediated activation of NADPH oxidases. *Sci Transl Med* 11: eaav5055

Bischoff J (2019) Endothelial-to-mesenchymal transition. *Circ Res* 124: 1163 – 1165

Chen PY, Qin L, Baeyens N, Li G, Afolabi T, Budatha M, Tellides G, Schwartz MA, Simons M (2015) Endothelial-to-mesenchymal transition drives atherosclerosis progression. *J Clin Invest* 125: 4514 – 4528

Derynck R, Zhang YE (2003) Smad-dependent and Smad-independent pathways in TGF-beta family signalling. *Nature* 425: 577 – 584

Forrester SJ, Booz GW, Sigmund CD, Coffman TM, Kawai T, Rizzo V, Scalia R, Eguchi S (2018) Angiotensin II signal transduction: an update on mechanisms of physiology and pathophysiology. *Physiol Rev* 98: 1627 – 1738

Gao J, Sun L, Huo L, Liu M, Li D, Zhou J (2010) CYLD regulates angiogenesis by mediating vascular endothelial cell migration. *Blood* 115: 4130 – 4137

Guo J, Wang Z, Wu J, Liu M, Li M, Sun Y, Huang W, Li Y, Zhang Y, Tang W *et al* (2019) Endothelial SIRT6 is vital to prevent hypertension and associated cardiorenal injury through targeting Nkx3.2-GATA5 signaling. *Circ Res* 124: 1448 – 1461

Harrigan JA, Jacq X, Martin NM, Jackson SP (2018) Deubiquitylating enzymes and drug discovery: emerging opportunities. *Nat Rev Drug Discov* 17: 57 – 78

Herhaus L, Al-Salihi M, Macartney T, Weidlich S, Sapkota GP (2013) OTUB1 enhances TGFbeta signalling by inhibiting the ubiquitylation and degradation of active SMAD2/3. *Nat Commun* 4: 2519

Huang YT, Cheng AC, Tang HC, Huang GC, Cai L, Lin TH, Wu KJ, Tseng PH, Wang GG, Chen WY (2021) USP7 facilitates SMAD3 autoregulation to repress cancer progression in p53-deficient lung cancer. *Cell Death Dis* 12: 880

Huang ZQ, Luo W, Li WX, Chen P, Wang Z, Chen RJ, Wang Y, Huang WJ, Liang G (2022) Costunolide alleviates atherosclerosis in high-fat diet-fed ApoE(−/−) mice through covalently binding to IKKbeta and inhibiting NF-kappaB-mediated inflammation. *Acta Pharmacol Sin* https://doi.org/10.1038/s41401-022-00928-0

Inoue Y, Imamura T (2008) Regulation of TGF-beta family signaling by E3 ubiquitin ligases. *Cancer Sci* 99: 2107 – 2112

Izzi L, Attisano L (2004) Regulation of the TGFbeta signalling pathway by ubiquitin-mediated degradation. *Oncogene* 23: 2071 – 2078

Jinnin M, Ihn H, Tamaki K (2006) Characterization of SIS3, a novel specific inhibitor of Smad3, and its effect on transforming growth factor-beta1-induced extracellular matrix expression. *Mol Pharmacol* 69: 597−607

Ju W, Ogawa A, Heyer J, Nierhof D, Yu L, Kucherlapati R, Shafritz DA, Bottinger EP (2006) Deletion of Smad2 in mouse liver reveals novel functions in hepatocyte growth and differentiation. *Mol Cell Biol* 26: 654−667

Komander D, Rape M (2012) The ubiquitin code. *Annu Rev Biochem* 81: 203−229

Kovacic JC, Dimmeler S, Harvey RP, Finkel T, Aikawa E, Krenning G, Baker AH (2019) Endothelial to mesenchymal transition in cardiovascular disease: JACC state-of-the-art review. *J Am Coll Cardiol* 73: 190−209

Laurent S, Boutouyrie P (2015) The structural factor of hypertension: large and small artery alterations. *Circ Res* 116: 1007−1021

Li J, Qu X, Yao J, Caruana G, Ricardo SD, Yamamoto Y, Yamamoto H, Bertram JF (2010) Blockade of endothelial-mesenchymal transition by a Smad3 inhibitor delays the early development of streptozotocin-induced diabetic nephropathy. *Diabetes* 59: 2612−2624

Li Z, Kong X, Zhang Y, Zhang Y, Yu L, Guo J, Xu Y (2020) Dual roles of chromatin remodeling protein BRG1 in angiotensin II-induced endothelial-mesenchymal transition. *Cell Death Dis* 11: 549

Lin K, Luo W, Yan J, Shen S, Shen Q, Wang J, Guan X, Wu G, Huang W, Liang G (2020) TLR2 regulates angiotensin II-induced vascular remodeling and EndMT through NF-kappaB signaling. *Aging (Albany NY)* 13: 2553−2574

Liu J, Jin J, Liang T, Feng XH (2022) To Ub or not to Ub: a regulatory question in TGF-beta signaling. *Trends Biochem Sci* 47: 1059−1072

Lu D, Song J, Sun Y, Qi F, Liu L, Jin Y, McNutt MA, Yin Y (2018) Mutations of deubiquitinase OTUD1 are associated with autoimmune disorders. *J Autoimmun* 94: 156−165

Ma J, Sanchez-Duffhues G, Goumans MJ, Ten Dijke P (2020) TGF-beta-induced endothelial to mesenchymal transition in disease and tissue engineering. *Front Cell Dev Biol* 8: 260

Massague J, Seoane J, Wotton D (2005) Smad transcription factors. *Genes Dev* 19: 2783−2810

Meng XM, Nikolic-Paterson DJ, Lan HY (2016) TGF-beta: the master regulator of fibrosis. *Nat Rev Nephrol* 12: 325−338

Mezzano SA, Ruiz-Ortega M, Egido J (2001) Angiotensin II and renal fibrosis. *Hypertension* 38: 635−638

Nan L, Jacko AM, Tan J, Wang D, Zhao J, Kass DJ, Ma H, Zhao Y (2016) Ubiquitin carboxyl-terminal hydrolase-L5 promotes TGFbeta-1 signaling by de-ubiquitinating and stabilizing Smad2/Smad3 in pulmonary fibrosis. *Sci Rep* 6: 33116

Oikawa D, Gi M, Kosako H, Shimizu K, Takahashi H, Shiota M, Hosomi S, Komakura K, Wanibuchi H, Tsuruta D *et al* (2022) OTUD1 deubiquitinase regulates NF-kappaB- and KEAP1-mediated inflammatory responses and reactive oxygen species-associated cell death pathways. *Cell Death Dis* 13: 694

Pardali E, Sanchez-Duffhues G, Gomez-Puerto MC, Ten Dijke P (2017) TGF-beta-induced endothelial-mesenchymal transition in fibrotic diseases. *Int J Mol Sci* 18: 2157

Piera-Velazquez S, Jimenez SA (2019) Endothelial to mesenchymal transition: role in physiology and in the pathogenesis of human diseases. *Physiol Rev* 99: 1281−1324

Popovic D, Vucic D, Dikic I (2014) Ubiquitination in disease pathogenesis and treatment. *Nat Med* 20: 1242−1253

Qian J, Luo W, Dai C, Wang J, Guan X, Zou C, Chattipakorn N, Wu G, Huang W, Liang G (2021) Myeloid differentiation protein 2 mediates angiotensin II-induced inflammation and mesenchymal transition in vascular endothelium. *Biochim Biophys Acta Mol Basis Dis* 1867: 166043

Rosenkranz S (2004) TGF-beta1 and angiotensin networking in cardiac remodeling. *Cardiovasc Res* 63: 423−432

Schiffrin EL, Touyz RM (2004) From bedside to bench to bedside: role of renin-angiotensin-aldosterone system in remodeling of resistance arteries in hypertension. *Am J Physiol Heart Circ Physiol* 287: H435−H446

Schluter KD, Wenzel S (2008) Angiotensin II: a hormone involved in and contributing to pro-hypertrophic cardiac networks and target of anti-hypertrophic cross-talks. *Pharmacol Ther* 119: 311−325

Senft D, Qi J, Ronai ZA (2018) Ubiquitin ligases in oncogenic transformation and cancer therapy. *Nat Rev Cancer* 18: 69−88

Song J, Liu T, Yin Y, Zhao W, Lin Z, Yin Y, Lu D, You F (2021) The deubiquitinase OTUD1 enhances iron transport and potentiates host antitumor immunity. *EMBO Rep* 22: e51162

Sorescu D (2006) Smad3 mediates angiotensin II- and TGF-beta1-induced vascular fibrosis: Smad3 thickens the plot. *Circ Res* 98: 988−989

Wang W, Huang XR, Canlas E, Oka K, Truong LD, Deng C, Bhowmick NA, Ju W, Bottinger EP, Lan HY (2006) Essential role of Smad3 in angiotensin II-induced vascular fibrosis. *Circ Res* 98: 1032−1039

Wang B, Cai W, Ai D, Zhang X, Yao L (2020) The role of Deubiquitinases in vascular diseases. *J Cardiovasc Transl Res* 13: 131−141

Wu B, Qiang L, Zhang Y, Fu Y, Zhao M, Lei Z, Lu Z, Wei YG, Dai H, Ge Y *et al* (2022) The deubiquitinase OTUD1 inhibits colonic inflammation by suppressing RIPK1-mediated NF-kappaB signaling. *Cell Mol Immunol* 19: 276−289

Wynn TA (2008) Cellular and molecular mechanisms of fibrosis. *J Pathol* 214: 199−210

Xia X, Liu X, Chai R, Xu Q, Luo Z, Gu J, Jin Y, Hu T, Yu C, Du B *et al* (2021) USP10 exacerbates neointima formation by stabilizing Skp2 protein in vascular smooth muscle cells. *J Biol Chem* 297: 101258

Xie F, Zhang Z, van Dam H, Zhang L, Zhou F (2014) Regulation of TGF-beta superfamily signaling by SMAD mono-ubiquitination. *Cell* 3: 981−993

Xu P, Duong DM, Seyfried NT, Cheng D, Xie Y, Robert J, Rush J, Hochstrasser M, Finley D, Peng J (2009) Quantitative proteomics reveals the function of unconventional ubiquitin chains in proteasomal degradation. *Cell* 137: 133−145

Yao F, Zhou Z, Kim J, Hang Q, Xiao Z, Ton BN, Chang L, Liu N, Zeng L, Wang W *et al* (2018) SKP2- and OTUD1-regulated non-proteolytic ubiquitination of YAP promotes YAP nuclear localization and activity. *Nat Commun* 9: 2269

Yegodayev KM, Novoplansky O, Golden A, Prasad M, Levin L, Jagadeeshan S, Zorea J, Dimitstein O, Joshua BZ, Cohen L *et al* (2020) TGF-beta-activated cancer-associated fibroblasts limit cetuximab efficacy in preclinical models of head and neck cancer. *Cancers (Basel)* 12: 339

Zeisberg EM, Tarnavski O, Zeisberg M, Dorfman AL, McMullen JR, Gustafsson E, Chandraker A, Yuan X, Pu WT, Roberts AB *et al* (2007) Endothelial-to-mesenchymal transition contributes to cardiac fibrosis. *Nat Med* 13: 952−961

Zhang J, Zhang X, Xie F, Zhang Z, van Dam H, Zhang L, Zhou F (2014) The regulation of TGF-beta/SMAD signaling by protein deubiquitination. *Protein Cell* 5: 503−517

Zhang Z, Fan Y, Xie F, Zhou H, Jin K, Shao L, Shi W, Fang P, Yang B, van Dam H *et al* (2017) Breast cancer metastasis suppressor OTUD1 deubiquitinates SMAD7. *Nat Commun* 8: 2116

Zhang L, Liu J, Qian L, Feng Q, Wang X, Yuan Y, Zuo Y, Cheng Q, Miao Y, Guo T *et al* (2018) Induction of OTUD1 by RNA viruses potently inhibits innate immune responses by promoting degradation of the MAVS/TRAF3/TRAF6 signalosome. *PLoS Pathog* 14: e1007067